THE JOURNAL OF PHYSICAL CHEMISTRY C

Article

pubs.acs.org/JPCC

Dewetting Dynamics of a Solid Microsphere by Emulsion Drops

Feng Lin,[†] Lin He,[†] Bauyrzhan Primkulov,[†] and Zhenghe Xu*[,†,‡]

[†]Department of Chemical and Materials Engineering, University of Alberta, Edmonton, Alberta T6G 2G6, Canada

[‡]Institute of Nuclear and New Energy Technology, Tsinghua University, Beijing, 100084, China

Supporting Information

ABSTRACT: A novel micropipet technique was developed to quantify the dewetting dynamics of individual microsphere particles by emulsified viscous crude oil drops in aqueous media. This technique allowed dynamic microscale receding contact angles of water to be measured in situ for solid−oil−water systems. System parameters, including modification of glass microspheres and characteristics of oil drops, were varied to study their effect on dewetting dynamics of the systems. Increasing solvent dosage in viscous oil was found to decrease static receding contact angle of water for clean and bitumen-treated glass surfaces, but showed a negligible effect on static receding contact angle for ethyl cellulose (EC)-treated glass surface. Interestingly, dynamic dewetting behavior exhibited a strong dependence on surface modification and the addition of solvent to viscous oil. No dewetting dynamics was observed for clean hydrophilic glass surface. For bitumen- or EC-treated glass surfaces, more rapid dewetting dynamics of water were determined with increasing addition of solvent to viscous oil. Both de Gennes viscous dissipation hydrodynamic and the Blake/Haynes molecular-kinetic models were developed for the current system to understand the observed dynamic dewetting characteristics.

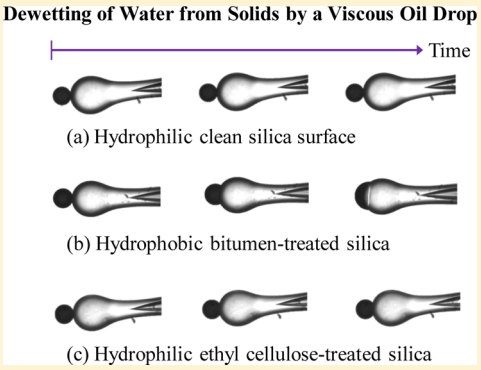

1. INTRODUCTION

When talking on wetting (or dewetting in the reverse direction), one might first consider the process of a single liquid spreading on a solid surface in a gaseous surrounding (mostly air), for example, as in the case of coating or printing. The wetting of this type (i.e., a one-liquid system) has been fairly well investigated for more than 50 years. However, many industrial and natural processes actually involve the displacement of one liquid by another immiscible liquid from a solid surface, that is, two-liquid wetting or dewetting. Important applications are seen in enhanced oil recovery,[1−3] detergency/cleaning,[4] oil−water filtration,[5] Pickering emulsion stabilization,[6] microfluidics,[7] biosurfaces,[8] mineral flotation,[9,10] bitumen extraction,[11,12] and wastewater treatment.[13,14] In addition to the significance of the extent that a solid is dewetted by the given liquid, also known as dewetting statics, one is often concerned with how fast the liquid can spread over a given area of a solid surface, that is, dewetting dynamics.

It is generally believed that the dewetting dynamics of one- or two-liquid systems are controlled by overall interactions, originating from surface, capillary, viscous, gravitational, inertia, and external forces, competing at three-phase contact line under dynamic conditions. Here, let us restrict to the simplest situation: the spontaneous displacement of one liquid by another on a solid surface with negligible gravity and inertia effect. Although the spreading process toward a new equilibrium in this case is commonly accepted as capillary driven, the energy dissipation mechanism involved remains an open debate. Depending on the mechanisms of energy dissipation, two different approaches have been used to explain the dewetting dynamics: molecular-kinetics and hydrodynamics. The first approach assumes that the dissipation is due to the attachment/detachment of liquid molecules to/from the solid, that is, molecular interaction, in the close vicinity of the triple contact zone, that is, the contact line friction. The second approach attributes the energy loss to viscous drag occurring in the core of the liquids. While both the contact line friction and the viscous dissipation account partially for the governing mechanisms of dynamic dewetting, the choice of the model depends largely on the characteristics of the system, particularly the viscosity range and velocity regime. The molecular-kinetic description has been shown to work fairly well for low viscosity liquids and/or slow contact line movements, that is, low capillary numbers.[10,15−17] On the other hand, the dewetting dynamics for the systems of high capillary number appear to be more appropriately captured by hydrodynamic models.[18−20] Recent studies have increasingly shown that the models considering both molecular-kinetics and hydrodynamics produce better agreement with experimental data than that considering only single dewetting mechanism.[21,22] The integration has, however, been largely phenomenological. As a result, there is a possibility of overparameterization, resulting in the loss of physical robustness of fitting parameters. It should be emphasized that the existing studies on dynamic dewetting have been restricted mainly to very limited cases of flow, mostly single-liquid systems. Blake,[23] de Gennes,[24] and de Coninck et

Received: December 27, 2013
Revised: May 12, 2014
Published: May 23, 2014

al.[25] provided comprehensive reviews on the subject. Clearly, the process of two-liquid dynamic dewetting is much more complex than its single-liquid counterpart. It is, therefore, no surprise that the issues of two-liquid dewetting dynamics remain poorly understood and require much further investigation.

To our knowledge, the most universal measure of the dewetting phenomena is perhaps by three-phase contact angle. In the past decades, numerous techniques of contact angle measurement have been developed. The common examples of these techniques include the sessile drop method that aligns a tangent with a drop shape profile at the point of three-phase contact circle and the Wilhelmy plate method, which determines the height of the rising or falling meniscus through proper illumination. It should be pointed out that these conventional methods usually require flat solid surfaces and drop sizes of more than 1 mm or well-defined capillaries. For this reason, most existing studies on dewetting are restricted to macroscopic systems. Details of these conventional methods together with their advantages and drawbacks were well described by Neumann and Good.[26]

In this study, we introduce a novel technique, micropipet, for measuring the contact angle on a micrometer size ball-shaped surface. This micropipet-based technique is designated to operate on the microscale and is much more realistic for characterizing the dewetting of fine particulates by emulsion liquid droplets. Rounded micropipet glass tips of micrometer sizes are chosen as model spherical solid substrates. Bitumen (i.e., highly viscous crude oil) and solvent-diluted bitumen dispersed in water are used as typical examples of emulsion oil droplets. With such oil-in-water emulsion systems, the interfacial tension and viscosity of oil emulsion droplets can be varied as desired. We will first describe in great detail the dynamics of individual oil emulsion droplets spreading on rounded glass micropipets of three different surface chemical properties (clean, bitumen-treated, demulsifier-treated) in water. The effects of two solvents (toluene and naphtha) addition to bitumen on both static and dynamic contact angles of glass/hydrocarbon/water systems are investigated. Two theoretical models based on the de Gennes hydrodynamics[24] and the Blake/Haynes molecular-kinetics,[23] respectively, are then derived for the current spherical systems and applied to describing and understanding the spreading dynamics of emulsion oil droplets on micrometer size glass sphere caps of variable wettability in water.

2. MATERIALS AND METHODS

2.1. Oil-in-Water Emulsions: Preparation and Measurement of Interfacial Tension. In this study, oil emulsions were prepared by introducing approximately 1 g of bitumen or diluted bitumen into 18 mL of water. The mixture was agitated in a sonication bath, creating emulsions of oil droplets that were 5−50 μm in diameter. In these emulsions, the dispersed phase is droplets of bitumen or diluted bitumen containing 10, 20, and 30 wt % of solvent, scaled by the amount of bitumen. Bitumen (the so-called "coker feed") was supplied by Syncrude Canada. ACS grade toluene (Fisher Scientific) and industry grade heavy naphtha (Champion Technologies) were used as dilution solvents. For the continuous (aqueous) phase, plant recycle process water from Syncrude Canada was used. The concentration of major ions in the process water was analyzed to contain 16 ppm magnesium, 26 ppm calcium, 24 ppm potassium, 656 ppm sodium, 128 ppm sulfate, 663 ppm chloride, 607 ppm bicarbonate, and 60 ppm natural surfactants (mainly carboxylic acids). The pH of the process water was adjusted, as required, to 8.0 ± 0.2 with 0.1 M sodium hydroxide or hydrogen chloride solution (both from Fisher Scientific), and measured using a digital pH probe (Accumet Research 20).

Oil−water interfacial tension σ_{ow} and viscosity of oil η_o depend strongly on the types and amounts of solvent added to bitumen. To characterize such an effect, viscosities η_o of bitumen and bitumen/solvent mixtures were measured via an AR-G2 rheometer (TA Instruments) at room temperature. The results are shown in Figure 1a. To determine the oil−water interfacial tension σ_{ow} of viscous fluids, the σ_{ow}/η_o ratio (the so-called characteristic velocity) was first determined using a drop shape recovery method developed by Moran et al.[27] In this method, σ_{ow}/η_o was obtained by adjusting this only unknown parameter to match the experimentally observed relaxation dynamics, that is, the axial length $L(t)$ as a function of shape recovering time t, of an extended drop with the Stokesian model. The results are shown in Figure 1b. From the values of oil viscosity η_o given in Figure 1a and the σ_{ow}/η_o ratio in Figure

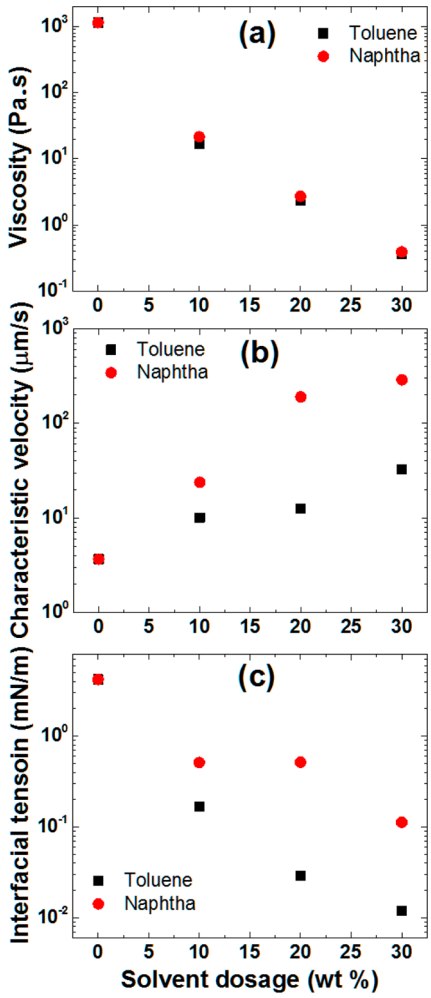

Figure 1. (a) Viscosity of oil (η_o); (b) characteristic velocity (i.e., interfacial tension to viscosity ratio σ_{ow}/η_o); and (c) oil−water interfacial tension σ_{ow}, as a function of the percentage of solvent addition to bitumen (scale by the weight of bitumen). Here, oil is bitumen or solvent-diluted bitumen. "■" points are toluene-diluted bitumen; red "●" points are naphtha-diluted bitumen.

1b, the interfacial tension σ_{ow} of oil emulsion drops could be obtained, as shown in Figure 1c.

2.2. Treatment of Glass Microsphere. As mentioned earlier, micrometer size spherical particles were obtained by melting the glass micropipets (details to be given in section 2.3). To control surface hydrophobicity of the glass microsphere, three different treatments were used. (1) The first was clean and untreated glass surface: To prevent contamination, rounded micropipets were prepared right before each experiment using glass capillary tubes as received from Fisher Scientific. The microspheres prepared as such were thought as "clean", as any organic impurity would have been decomposed and vaporized much earlier before reaching the glass melting temperature. (2) The second was bitumen-coated surface: To prepare the surfaces of controllable charges and hence variable hydrophobicities,[28] the prepared clean glass microspheres using method (1) were dipped completely in toluene-diluted bitumen at a bitumen to toluene mass ratio of 3:1 for 2 days to ensure equilibrium conditions. The microspheres were then washed with toluene and dried at room temperature in a dust-free laminar clean hood. (3) The final was demulsifier-treated surface: To mimic the washing of contaminated sand grains, the bitumen-treated glass microspheres were dipped in a toluene solution of 1 wt % water-insolvable ethyl cellulose (EC, with 48% ethoxyl and viscosity of 4 cP, Sigma-Aldrich) as demulsifier, for overnight at room temperature.[29] The treated samples were repeatedly washed with toluene to ensure that the remaining EC was irreversibly adsorbed on the solid surface, which could not be washed off by toluene, and then dried in air by natural evaporation.

2.3. Static and Dynamic Dewetting. Micropipet technique was applied to investigate the interactions between individual emulsion oil droplet and a solid particle. A photograph of such an "interaction test" is shown in Figure 2. Micropipet technique was initially put forward by Yeung and his co-workers into the research of emulsions.[30] In this study, this technique was further modified to prepare a close-ended glass micropipet of spherical shape.

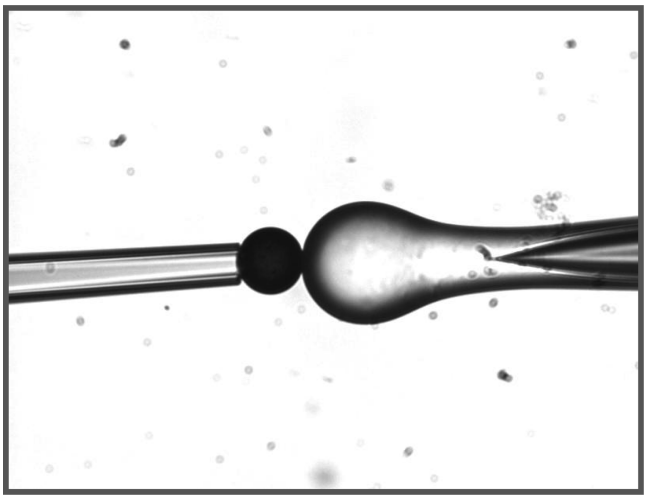

Figure 2. Oil−solid contact experiment: an individual oil droplet of diameter close to 40 μm (left), chosen from a pool of emulsified oil droplets dispersed in the continuous aqueous medium known as "industrial process water", is being brought in contact with a microspherical glass surface (right) and allowed to spread until the final configuration (shape) is reached. The presence of the remaining emulsified oil droplets as shown in the background aqueous medium has no impact on the experiment. Video clips describing the spreading processes are provided in the Supporting Information.

A schematic of the micropipet experiment system is shown in Figure 3. The micropipets were made from capillary tubes (Drummond Scientific). Using a hot wire pipet puller (Kopf, model 730), individual capillary tubes were stretched axially under high temperature, producing two separate sections with tapered ends. To obtain a smooth open-ended tip with typical inner diameter of 10−15 μm, the tapered pipet tip was truncated with a homemade forging apparatus. To produce a rounded closed tip, the tapered end of the capillary was melted by a hot platinum wire, forming a closed end of truncated sphere. The diameter of the truncated sphere was controlled to about 65−70 μm. Before each experiment, the micropipets of truncated spheres were pretreated as described in section 2.2.

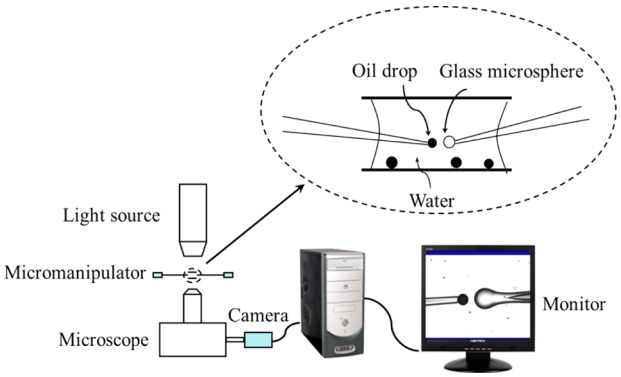

Figure 3. Schematics of micropipet experimental setup. As seen in the monitor image (an actual photograph), individual emulsified oil droplets in water inside the sample cell (also shown in the blow-up view) are captured by the micropipet on left; the micropipet on the right, with a closed and rounded tip, functions as a spherical glass particle.

Drops of oil-in-water emulsion (about 2 mL) were placed in a small glass cell of hydrophilic surface to avoid the spreading of the emulsions on the cell wall. Two micropipets were immersed into the emulsion through the open sides of the cell. The micropipet on the left was open-ended. The large end of this micropipet was connected to a suction line through flexible tubing attached to a high precision micrometer syringe pump. This micropipet was used to pick up and hold an emulsified oil droplet with the suction pressure adjusted by the syringe pump. The micropipet on the right was close-ended with a truncated spherical shape. The sphere at the end of this micropipet functioned as solid (glass) particles of variable surface properties. Both micropipets were mounted on hydraulic manipulators, which enabled the smooth and microscale displacement of the micropipets. The interactions between the oil drop and the glass particle approaching each other were monitored in situ under an inverted optical microscope (Zeiss Axiovert 200). The approaching process was recorded by a digital camera interfaced with personal computer. The still images were used for contact angle measurements. In our experiments, oil droplets of 38 μm average diameter with less than 5% variations were picked up from a large selection of an emulsion pool with the aid of "electronic calipers".

With the above-mentioned settings, oil-solid contact experiments were carried out by gently bringing an individual oil droplet at the tip of open-ended micropipet to contact the

truncated glass sphere surface (pipet on right in Figure 2). Once they touched with each other, the oil droplet would, under favorable conditions, spread spontaneously over the glass surface until the system reached an equilibrium configuration where the three-phase contact point and shape remained unchanged with time. From the recorded image, the angle between two tangent lines drawn at the three-phase contact point was measured from the aqueous phase using built-in image analysis software Image Pro and referred to as the receding contact angle (θ_d) of water by the displacement of the advancing oil droplet on the spherical glass surface. The angles at both the top and the bottom contact points were measured to ensure the consistency of the measurements. All of the measurements were carried out at room temperature (22.5 ± 1 °C), and repeated for each condition at least five times with good reproducibility. To study the dynamic effect, each dewetting process was preceded for a duration of up to 30 min. For each droplet observed, the receding contact angle at any instant analyzed (known as dynamic receding contact angle) was plotted as a function of dewetting time. The experimental values of these dynamic receding contact angles were compared to the theoretical predictions of the models described in the next section.

We emphasize here several advantages that the micropipet offers over the conventional and macroscopic (i.e., millimeter-scale) methods such as the commonly used sessile drop method. The new technique is best suited for the direct and in situ quantification of liquid–liquid displacement on the microscale. It can be easily applied to study of dewetting (or wetting) behaviors of an individual colloidal particle (or powder), overcoming the limitations that only an averaged contact angle value is obtained by conventional methods. Using the micropipet, the sizes of liquid droplet and solid particle can be well selected/controlled. Furthermore, the micropipet technique minimizes the influence of the gravity and consequently the distortion of the profile of the micrometer size liquid droplets. For systems with liquids of different densities, the outcome of the micropipet experiments dose not depend on whether the dispersed phase is denser or lighter. In addition, this new method requires much smaller volumes of dispersed liquid, which could be a limiting factor for the experiments where only a trace amount of liquid is available. Because of the use of transmission bright-field illumination embedded in an inverted microscope, the micropipet method is more tolerable to the opacity of the continuous liquid phase as compared to the sessile drop technique in which the continuous phase needs to be transparent to get clear and sharp interfacial contours.

3. THEORY OF DEWETTING DYNAMICS

As described above, the spreading of oil to replace water over a solid surface, investigated in this study, is spontaneous. For the drops of micrometer sizes, the gravitational and the inertial effects can be safely ignored due to their extremely small values of the Bond number (ratio of gravitational to capillary forces, $B_o \approx 10^{-3}$ or less) and the Weber number (ratio of inertial to capillary forces, $W_e \approx 10^{-9}$ or less). The spreading process is therefore driven by the capillary force. The imbalance of interfacial tensions drives the displacement of water by oil droplet. For the contact angle measured through the aqueous phase, the driving force (F_A) exerting on the oil droplet at triple contact line is written as[20,24]

$$F_A = \sigma_{ow}[\cos(\pi - \theta_e) - \cos(\pi - \theta_d)] \quad (1)$$

where σ_{ow} is oil–water interfacial tension, θ_e is the equilibrium receding water contact angle with $(\pi - \theta_e)$ representing the equilibrium advancing contact angle measured through the oil phase, and θ_d is the dynamic receding water contact angle at time t.

Depending on the energy dissipation mechanism that balances the action of capillary force, two distinct approaches, molecular-kinetic and macroscopic hydrodynamic, have been used to model the contact angle dynamics. Numerical studies[21,23,25,31−35] suggested that a given set of the experimental dynamic dewetting data could be often fitted by one model as successfully as by another. In this study, we will apply the two most commonly used models to our current micro spherical systems and fit our experimental data with these two models. Our interest is to further illustrate the critical role of physicochemical properties of the system, such as liquid viscosity and interfacial tension, in determining spreading dynamics of emulsion droplets on micrometer size glass sphere caps of variable wettability in water.

Hydrodynamic. When applying the macroscopic hydrodynamic (HD) theory to modeling dewetting dynamics, the nonslip condition at the fluid/fluid interface on a solid surface in the conventional continuum theory has to be relaxed, at least at a molecular length scale to allow for finite slippage of the interface on solid surfaces. Several strategies have been employed by different investigators to account for the required slippage.[36−39] Among them, the model proposed by de Gennes[24] exploited the well-known "lubrication approximation" of fluid mechanics to describe the viscous dissipation in an advancing liquid front by excluding the small cutoff region from the analysis. This model has been shown to successfully rationalize the dynamic wetting or dewetting behaviors for a wide range of systems, in particular those on a flat substrate.[40] Recently, Basu et al.[20] applied this model successfully to describe the dewetting process of a bitumen/water/(flat) glass surface system. Here, we will adopt the basic framework of de Gennes' theory for viscous dissipation, and present a working model to describe the dynamic dewetting of a spherical solid surface by an emulsion oil droplet in water.

During the dewetting process of water by a more viscous fluid (in this case, bitumen or diluted bitumen) from a spherical solid surface, viscous dissipation mainly occurs in the core of oil droplet (not in water). The viscous force (F_V) per unit length of contact line, from the derivation of de Gennes,[24] is given by

$$F_V = \left(\frac{3\eta_o}{\pi - \theta_d}\right) v \ln(\varepsilon_\delta^{-1}) \quad (2)$$

where η_o is the viscosity of oil and $\pi - \theta_d$ is the advancing dynamic contact angle measured from oil phase at time t. ε_δ in eq 2 is a dimensionless number given by $\varepsilon_\delta = x_\delta/x_{max}$, where x_δ is the molecular scale cutoff length and x_{max} is the characteristic length of the spreading drop, that is, the diameter of oil drop in this case. In eq 2, the viscous effect at the smaller distance than x_δ is neglected from hydrodynamic analysis.[24,31] v in eq 2 is instantaneous contact line displacement velocity at time t, which is simply the derivative of the arc OB (expressed as l, with O being the central point of oil–solid contact line and B being the three-phase contact (TPC) point: see Figure 4 for the description) over time t:

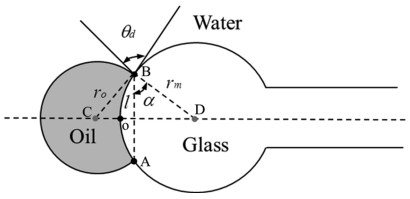

Figure 4. Schematic view of an oil droplet when attached on a spherical solid particle.

$$v = \frac{dl}{dt} \tag{3}$$

If we consider the balance of the viscous dissipation by the capillary driving force (i.e., equating eqs 1 and 2), rearranging this equality together with eq 3 leads to the following equation for contact line velocity (v):

$$v = \frac{dl}{dt} = \frac{(\pi - \theta_d)}{3\ln(\varepsilon_\delta^{-1})}\left(\frac{\sigma_{ow}}{\eta_o}\right)(\cos\theta_d - \cos\theta_e) \tag{4}$$

Because of the negligible gravitational and inertial effects during the dewetting (or oil spreading) process, the geometry for the attached section of the solid by the oil is a spherical cap, while the shape of the oil droplet could be considered as a truncated sphere, as shown in Figure 4. Spreading of the oil droplet on the spherical solid surface generates different contact angles. However, the volume of the oil droplet is constant during the spreading process due to the two facts that (1) the oil we studied, bitumen or diluted bitumen, is immiscible with water and of a negligible solubility in water, and (2) there is no break-off of the oil droplet during the spreading. These assumptions (including the shape of oil droplet and solid sphere) have been clearly validated with the images of the dewetting process. With these assumptions, the conservation equation of oil volume (V) in spherical coordinate system is written as

$$V = \frac{\pi}{3}r_o^3[2 + 3\sin(\alpha + \theta_d) - \sin^3(\alpha + \theta_d)] - \frac{\pi}{3}r_m^3(2 - 3\sin\alpha + \sin^3\alpha) = \frac{4\pi}{3}r_{o,i}^3 \tag{5}$$

where r_o is the radius of the spherical cap in the oil phase (the length CB); r_m is the radius of the spherical glass particle (the length BD); and α the angle between the vertical axis (BA) and the line (BD) connecting the TPC point (B) and central point (D) of the glass sphere. The visual descriptions of r_o, r_m, and α are shown in Figure 4. $r_{o,i}$ in eq 5 is the radius of the initial oil drop before the oil touches solid surface.

Essentially, the angle α, related to dynamic contact angle θ_d via eq 5, is also a function of the arc l and the radius r_o. Initially, as the oil spreads, both the arc l and the dynamic receding contact angle θ_d increase, while the angle α decreases. From geometrical consideration, the arc l and the radius r_o can be expressed as

$$l = r_m(\pi/2 - \alpha) \tag{6}$$

$$r_o = r_m\cos\alpha/\cos(\pi - \alpha - \theta_d) \tag{7}$$

By substituting eq 7 into eq 5 and differentiating eqs 5 and 6 in combination with eqs 4 and 7, the following two useful relations are obtained:

$$\frac{\cos^3\alpha}{\cos^3(\pi - \alpha - \theta_d)}[2 + 3\sin(\alpha + \theta_d) - \sin^3(\alpha + \theta_d)] - (2 - 3\sin\alpha + \sin^3\alpha) = 4\left(\frac{r_{o,i}}{r_m}\right)^3 \tag{8}$$

$$\frac{d\theta_d}{dt} = \frac{(\pi - \theta_d)}{3r_m\ln(\varepsilon_\delta^{-1})}\left(\frac{\sin\theta_d}{\cos\alpha}\right)[2 - \sin(\alpha + \theta_d)]\left(\frac{\sigma_{ow}}{\eta_o}\right)(\cos\theta_d - \cos\theta_e) \tag{9}$$

In eqs 8 and 9, the radii of the solid sphere and the initial oil droplet, r_m and $r_{o,i}$, are known precisely. In the current study, they are controlled to be 34 and 19 μm, respectively, with a range in size less than ±5%. Two boundary conditions, that is, initial and equilibrium of contact angle, $\theta_d(t = 0) = \theta_i$ and θ_e, are measured experimentally from still images. The value of σ_{ow}/η_o is also experimentally determined using the drop shape recovery method (results shown in Figure 1b) applied to emulsion drops of similar sizes. Therefore, there is only one undetermined variable, ε_δ, in the present model. In the current study, this variable ε_δ is adjusted to curve fit the model with the experimentally measured dynamic contact angles.

Unfortunately, there is no analytical solution to integration of eqs 8 and 9. Mathematically, for a given ε_δ, eqs 8 and 9 can be solved numerically using an ODE package to calculate the dynamic contact angles θ_d at a given time t for each condition. The least-squares of the differences between the measured and calculated dynamic contact angles, Ψ, is then calculated by

$$\Psi \equiv \sum_{t=0}^{t_e}[\theta_{d,t}(\text{theoretical}) - \theta_{d,t}(\text{experimental})]^2 \tag{10}$$

The summation runs from 0 to t_e (i.e., the time from the initial contact to the equilibrium state). By minimizing Ψ with respect to ε_δ, we obtain the optimal value of the parameter ε_δ, which can be used to predict the dewetting dynamics, that is, dynamic contact angles. Note that if the planar glass surface is used as in the conventional sessile drop method, the angle α approaches to $\pi/2$, and the arc l becomes the base radius of the oil droplet attached to planar surface. As a result, the instantaneous change of contact angle in the HD model (i.e., eq 9) becomes[20]

$$\frac{d\theta_d}{dt} = \frac{(\pi - \theta_d)}{3l\ln(\varepsilon_\delta^{-1})}\sin\theta_d[2 - \sin(\pi/2 + \theta_d)]\left(\frac{\sigma_{ow}}{\eta_o}\right)(\cos\theta_d - \cos\theta_e) \tag{11}$$

Molecular-Kinetic. The molecular-kinetic (MK) theory was first proposed by Blake and Haynes to describe the wetting or dewetting dynamics.[15] Details of the MK theory can be found elsewhere.[17,21,23,25] Here, we will give a brief description of applying the MK theory to our current spherical system. As originally conceived, the dissipation channel for the macroscopic moving contact line is dictated by the statistics of molecular displacements (jumps) that occurred in close vicinity of contact line when viewed at the molecular level. The work to overcome the thermal energy barrier of these jumps is provided by the unbalanced interfacial tensions. If each jump is characterized by a characteristics length λ and an equilibrium frequency k^0, then the velocity of the contact line displacement v is given by

$$v = 2\kappa^0\lambda \sinh[\sigma_{ow}(\cos\theta_d - \cos\theta_e)/(2\lambda^{-2}k_BT)] \quad (12)$$

where k_B is the Boltzmann constant and T is the absolute temperature. By considering the spherical geometry as mentioned earlier, the instantaneous change of contact angle for our current system is expressed as

$$\frac{d\theta_d}{dt} = \frac{1}{r_m}\left(\frac{\sin\theta_d}{\cos\alpha}\right)[2 - \sin(\alpha + \theta_d)](2\kappa^0\lambda) \sinh[\sigma_{ow}(\cos\theta_d - \cos\theta_e)/(2\lambda^{-2}k_BT)] \quad (13)$$

If the argument of the sinh function is small, for example, σ_{ow} is small or θ_d is close to θ_e, eqs 12 and 13 can be simplified to the linear form of eqs 14 and 15, respectively:

$$v = \left(\frac{\sigma_{ow}}{\zeta}\right)(\cos\theta_d - \cos\theta_e) \quad (14)$$

$$\frac{d\theta_d}{dt} = \frac{1}{r_m}\left(\frac{\sin\theta_d}{\cos\alpha}\right)[2 - \sin(\alpha + \theta_d)]\left(\frac{\sigma_{ow}}{\zeta}\right)(\cos\theta_d - \cos\theta_e) \quad (15)$$

where $\zeta = k_BT/(k^0\lambda^3)$ is the coefficient of contact-line friction. Similarly, λ and k^0 or ζ are treated as adjustable parameters and obtained by curve fitting to the experimental data of dynamic contact angle at a given condition. For planar glass surface, the rate of contact angle change in the linear MK model (i.e., eq 15) can be written as

$$\frac{d\theta_d}{dt} = \frac{1}{l}\sin\theta_d[2 - \sin(\pi/2 + \theta_d)]\left(\frac{\sigma_{ow}}{\zeta}\right)(\cos\theta_d - \cos\theta_e) \quad (16)$$

In the above equations of the dewetting models, the units of static and dynamic contact angles are in radian. The contact angles are expressed in degrees in the actual curve fitting to the experimental data.

4. RESULTS AND DISCUSSION

The equilibrium dewetting state of water by emulsion oil droplets on a spherical glass surface of three different treatments is discussed first, followed by discussions on dynamic dewetting phenomena of these same systems. The dewetting models developed above are then applied to fit and predict the dynamic contact angles measured experimentally.

4.1. Equilibrium Contact Angle. The measured equilibrium contact angles for micro glass/oil/water systems are shown in Figure 5. It is evident that the clean and untreated glass surfaces were hydrophilic, as indicated by the receding water equilibrium contact angles of much less than 90° shown in Figure 5a. However, for bitumen-treated glass surfaces, the equilibrium contact angles were in the range of over 90° as shown in Figure 5b. This finding implies that bitumen had the ability to contaminate the glass surface, making it hydrophobic. Because the clean glass microspheres were dipped in toluene-diluted bitumen and then washed with toluene to prepare the bitumen-treated surfaces, the treated surfaces contained a layer of irreversibly adsorbed bitumen components such as resins and asphaltenes. The polar nature of these components containing polyaromatic rings with oxygen-, sulfur-, and/or nitrogen-heteroatoms[41] allowed them to bind through hydrogen bonding with the hydroxyl groups on clean glass surface in toluene, accounting for the irreversible contamination of the glass sphere by these components and hence increased hydrophobicity.

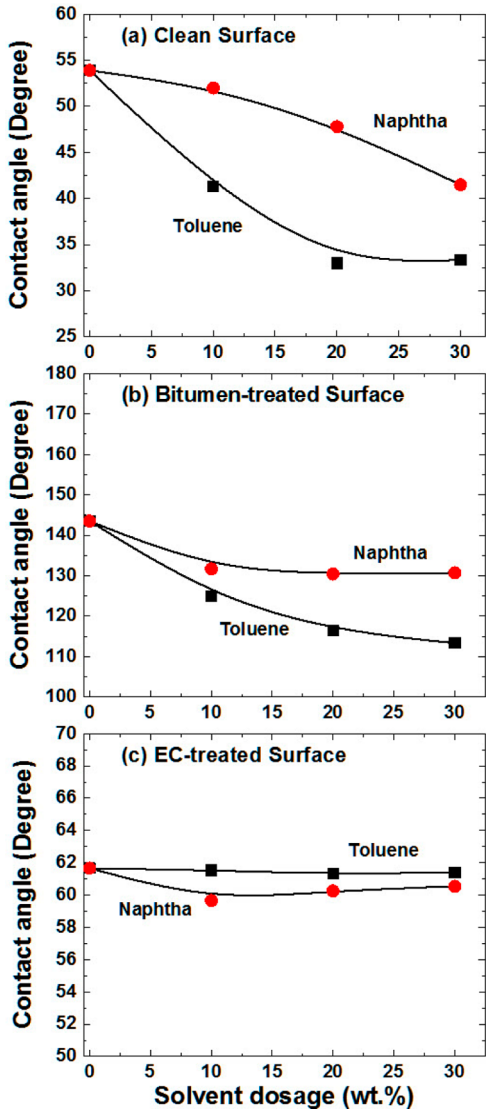

Figure 5. Equilibrium receding contact angle of water on (a) clean glass surface; (b) bitumen-treated glass surface; and (c) EC-treated glass surface, as a function of solvent dosage in bitumen (scaled by the weight of bitumen). "■" points represent the toluene addition, while red "●" points represent the naphtha addition to diluted bitumen as the spreading oil droplets. The solid line is a spline fit to the data points.

The results in Figure 5a and b also show a significant decrease in receding contact angle for both clean and bitumen-treated glass surfaces, when the surface is dewetted by bitumen diluted with an increasing amount of solvent in bitumen. For a given solvent dosage, the reduction in the equilibrium receding contact angle by toluene addition is more significant than by naphtha addition. Interestingly, such observation corresponds well to a more significant reduction in both viscosity and interfacial tension of diluted bitumen by toluene addition than by naphtha addition, as shown in Figure 1.

After the bitumen-treated glass surfaces were washed with demulsifier EC in toluene solution, the equilibrium receding contact angles were reduced to about 60° as shown in Figure 5c, suggesting that EC was able to modify the bitumen-treated glass surfaces from oil-wet to water-wet. The result suggests

that demulsifier EC could at least competitively adsorb and/or displace, if not completely, the bitumen components that already anchored on the glass surface. This high displacement activity of hydrocarbon contaminants from solid interface by EC has been reported in recent studies.[29,42,43] Using quartz crystal microbalance with dissipation (QCM-D) and atom force microscopy (AFM), for example, Wang et al.[29] detected the irreversible adsorption of EC on asphaltenes- and bitumen-tainted silica or alumina. Interestingly, Figure 5c shows that the addition of each solvent (toluene or naphtha) had a negligible effect on the equilibrium receding contact angles for EC-treated glass surfaces. Such an observation is attributed to the strong and irreversible adsorption of EC on the glass surface.[29]

4.2. Dynamic Contact Angle. Three series of photographs in Figure 6 illustrate the effect of surface hydrophobicity on

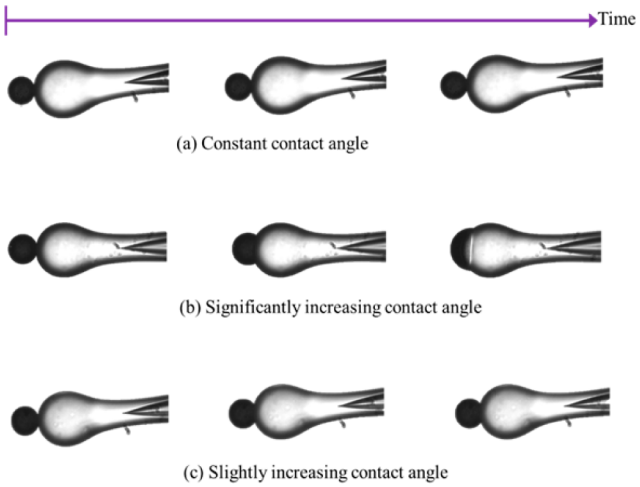

Figure 6. (a) Constant water contact angle for clean glass surface; (b) significantly increasing water contact angle for bitumen-treated glass surface; and (c) slightly increasing water contact angle for EC-treated glass surface, with increasing contact time of viscous oil drop with glass sphere in plant process water of pH 8.

dewetting dynamics of water from the spherical glass surfaces by an oil drop. Figure 6a shows an oil droplet sitting on the hydrophilic clean glass surface in industrial process water. No obvious dewetting was observed for this hydrophilic glass surface. At the given experimental condition, the contact angle remained constant as the contact continued right after the breach of oil−water interfaces and rapid establishment of three-phase contact lines. (Also see SI_movie 1 of the Supporting Information.) In contrast to the hydrophilic clean glass surface, obvious contact line movement was seen, and the contact angle of receding water increased with increasing the contact time of the oil droplet on the bitumen- or EC-treated glass surfaces, as shown in Figure 6b and c. (Also see SI_movie 2 and SI_movie 3 of the Supporting Information.) In this case, the velocity of the contact line movement was found to decrease with time as the contact angle approached the equilibrium value.

Quantitative descriptions of dynamic contact angles θ_d as a function of spreading time of the oil on bitumen- and EC-treated glass surfaces are shown in Figures 7 and 8, respectively. Effect of solvent type (toluene and naphtha) on the change of dynamic contact angle was investigated. Similar to the contact line movement at a given condition on two substrates, the dynamic receding water contact angles were initially increased rapidly, then relaxed and finally plateaued to an equilibrium

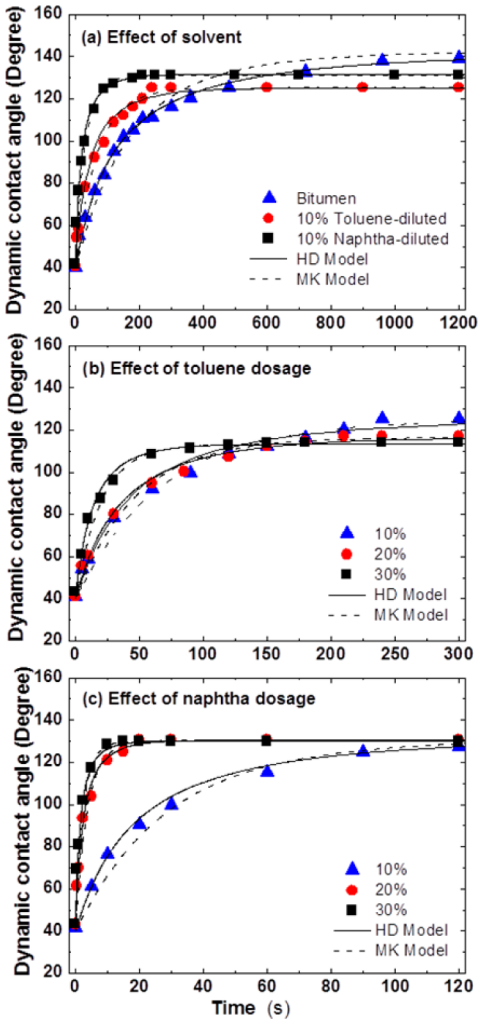

Figure 7. Dynamic contact angles of the emulsion oil drops spreading on bitumen-treated surface as a function of time. Here, the symbols are the results of experimental contact angle measurements. The solid lines are HD theoretical predictions based on the same best fitted parameter value of $\varepsilon_\delta = 0.0001$. The dashed lines are the predictions of linear MK model according to the respective ζ values shown in Figure 10. To reflect a different time scale for reaching the equilibrium contact angle and avoid overcrowding of information, the data are plotted in three main aspects: (a) effect of solvent (i.e., bitumen, 10 wt % toluene-, or 10 wt % naphtha-diluted bitumen); (b) effect of toluene dosage at 10, 20, and 30 wt %; and (c) effect of naphtha dosage at 10, 20, and 30 wt %.

value. The change in dynamic contact angle was found to be more rapid with increasing the dosage of the solvent added to the bitumen, reducing the time required for dewetting to reach equilibrium state. On a given glass surface at the same level of solvent addition, the dewetting of water by diluted bitumen was found to be faster with naphtha addition than with toluene addition. For the same oil, it took longer time to attain the zero velocity state (i.e., equilibrium receding contact angle) on bitumen-treated (hydrophobic) glass surface than on EC-treated (hydrophilic) glass surface.

4.3. Model Verification of Dynamic Contact Angle. *Hydrodynamic.* As described in section 3, the HD model developed has one free (unknown) parameter: the normalized molecular scale cutoff length ε_δ, while the combined parameter σ_{ow}/η_o, the oil−water interfacial tension to oil viscosity ratio,

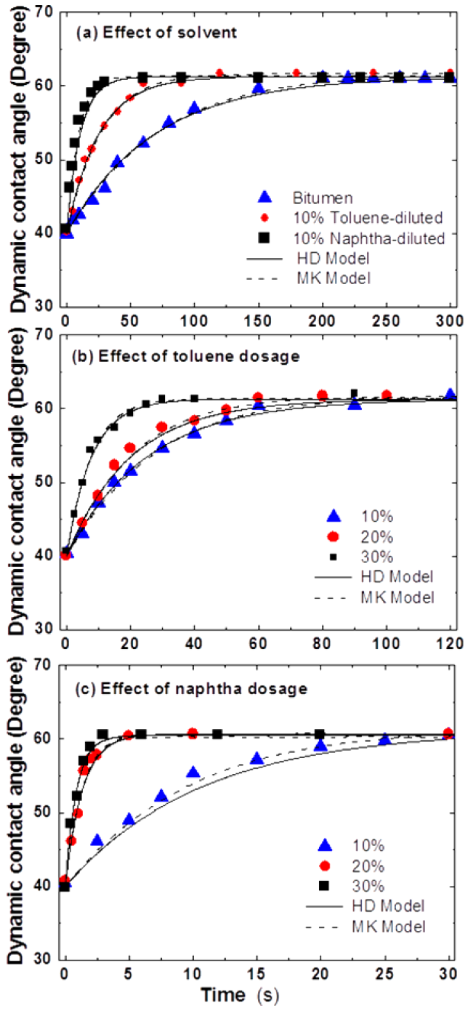

Figure 8. Dynamic contact angles of the emulsion oil drops spreading on EC-treated surface as a function of time. Here, the symbols are the results of experimental contact angle measurement. The solid lines are HD theoretical predictions based on the same best fitted parameter value of $\varepsilon_\delta = 0.01$. The dashed lines are the predictions of linear MK model using the respective ζ values shown in Figure 10. To reflect a different time scale for reaching equilibrium contact angle and avoid overcrowding of information, the data are plotted in three main aspects: (a) effect of solvent (i.e., bitumen, 10 wt % toluene-, or 10 wt % naphtha-diluted bitumen); (b) effect of toluene dosage at 10, 20, and 30 wt %; and (c) effect of naphtha dosage at 10, 20, and 30 wt %.

can be determined experimentally as shown in Figure 1b. In this study, the free parameter ε_δ is determined by the minimization of the least-squares functional as defined in eq 10 for one oil spreading on each surface. For spreading of bitumen droplets, the resulting ε_δ value is 0.0001 for bitumen-treated surface and 0.01 for EC-treated surface. These values are used in predicting dewetting dynamics of corresponding solid surface systems.

The solid lines in Figures 7 and 8 represent the HD theoretical curves of dynamic contact angles obtained through the integration of eqs 8 and 9 using the above fitted ε_δ values for corresponding solid surfaces. Because the difference in the experimentally measured initial contact angles for all of the conditions was less than 2%, all of the theoretical curves (i.e., solid lines) started from the same initial point. As can be seen, the applicability of the de Gennes hydrodynamic model to interpreting the dynamic contact angles is remarkable. Most significantly, the hydrodynamic model allows us to identify the significance of the three critical controlling parameters in dewetting dynamics: oil−water interfacial tension, viscosity of oil droplet, and solid surface hydrophobicity.

It is worth verifying the validity of the hydrodynamic model in predicting the initial velocity (v_o) of TPC displacement. This initial velocity at a given condition is calculated with eq 4 at time zero ($t = 0$), and plotted against the σ_{ow}/η_o ratio for two substrates, by solid lines in Figure 9. Experimentally, the initial

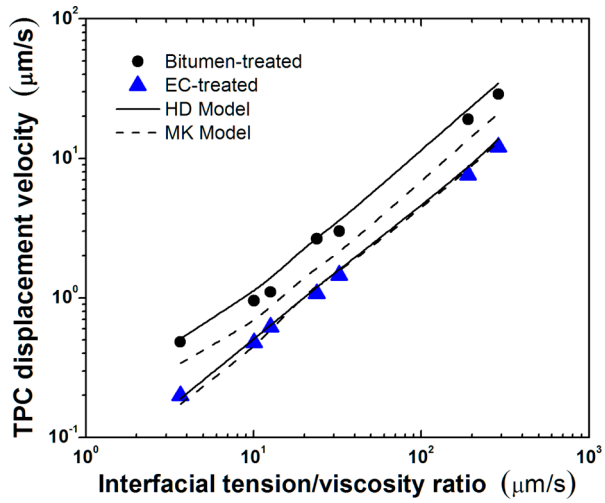

Figure 9. Initial velocity of contact line displacement as a function of interfacial tension to viscosity ratio on two substrates. The symbols are the results of experimental contact line velocity measurements, and solid lines are theoretical predictions based on eq 4 (HD model) at time zero. The dashed lines are predictions of linear MK model based on eq 14 at initial time.

contact line displacement velocity was estimated from the recorded images as the measured initial displacement of three-phase contact line on the arc divided by the small time interval of measurement. The experimental results are shown as the symbols in Figure 9. The quality of agreements between these theoretical and experimental values further reinforces the validity of the de Gennes HD theoretical model. As demonstrated in Figure 9, the initial contact line displacement rate on a given substrate is almost linearly proportional to the σ_{ow}/η_o ratio (which was controlled by the dosage of solvent to bitumen). Clearly, the rate of initial TPC displacement for the same oil (i.e., the identical σ_{ow}/η_o ratio) was higher on hydrophobic bitumen-treated substrate than on hydrophilic EC-treated substrate. This fundamental study provides a sound guidance on enhancing displacement rate by formulating the displacement fluid of increased interfacial tension and/or reduced viscosity.

It is also interesting to comment on the parameter ε_δ, which represents the dimensionless scale for normalized cut off region. Let us consider the two extreme cases. The system of $\varepsilon_\delta = 0$ corresponds to "non-slip" condition (or no cutoff) of zero fluid velocity at the surface. In such system, there is no mass flux of fluid across the solid−liquid interface. The dissipation in this case would diverge to the state that "not even Herakles could sink a solid", as interpreted by Hub and Scriven.[39] The condition of $\varepsilon_\delta = 1$ refers to the case of unimpeded tangential slip between fluid and solid. A small value of ε_δ between [0, 1] corresponds to a system with the formation of a displacing fluid−solid interface while eliminating an existing fluid−solid

interface as the TPC line advances. The large variation in the best fitted value of ε_δ suggests that the ε_δ is highly dependent on the solid surface properties with the value for the hydrophobic bitumen-treated surface being 2 orders of magnitude smaller than that for hydrophilic EC-treated surface. The properties of oil (bitumen diluted with a varying amount of solvent) have a negligible effect on ε_δ as shown by a near perfect fit of the experimental results with the model without changing the value of ε_δ. It is shown from eq 9 that the fitting parameter ε_δ has only a weak (logarithmic) effect on the dynamic contact angle. Because the molecular scale cutoff length (x_δ) is the product of ε_δ and the characteristic length of the spreading drop (i.e., the diameter of the oil drop), with similar diameters of the initial oil droplets used in this study, x_δ is estimated in the order of magnitude to be 1 nm for bitumen-treated glass surface and 100 nm for EC-treated surface. The descriptions of the experimental receding dynamic contact angle data by the Cox−Vionov hydrodynamic model[37] are not presented here due to the significantly poor fit of the data to the model.

Molecular-Kinetic. For the full version of the MK model, multiple solutions for two fitting parameters λ and k^0 would be generated. Because the interfacial tensions in our systems, as shown in Figure 1c, are low, the linear MK model containing one adjustable parameter ζ is employed. Similar to the earlier treatment in the HD model, the regression is done by an initial guess of ζ and a simultaneous integration of eqs 15 and 8, then seeking the values that best fit to experimental data at a given condition, minimized by the least-squares of sum (i.e., eq 10 with respect to ζ). In most cases, the predictions from the linear MK model, as indicated by the dashed lines in Figures 7 and 8, also agree reasonably well with the measured receding water contact angle values. In the case of a bitumen drop spreading on the bitumen-treated glass surface, the fit to the linear eq 15 is poor, but the fit was adequate to the full MK eq 13.

The corresponding values of the fitting parameter ζ in the MK model are presented as symbols in Figure 10. Evidently, the contact line friction, ζ, of oil−water interface against the micro glass surface is proportional to the viscosity of the spreading oil, depending on the inherent characteristics of glass surface. For the same surface, the log−log plot of ζ against η_o is indeed linear with a slope of 1: a high viscosity leads to a high friction. This finding has obvious implications for the interfacial diffusion and reorganization process that occurred in the TPC zone.[44] In addition, the friction for the same oil (i.e., the identical η_o) is larger on hydrophobic bitumen-treated surface than on hydrophilic EC-treated counterpart. A higher ζ value for the same oil−water interface corresponds to a stronger solid−liquid interaction, and vice versa. Considering the two competing trends,[17] our results suggest that in our two-liquid systems, the influence of the viscous oil−solid interaction dominates over the water−solid interaction. On the basis of the linear correlation between ζ and η_o, the application of the MK model to our current system also confirms that the liquid−liquid displacement rate is largely controlled by the interfacial tension to viscosity ratio, that is, by the σ_{ow}/η_o ratio.

The dashed lines in Figure 9 show the initial velocities predicted by the linear MK model of eq 14 at initial time. Interestingly, for bitumen-treated surface, the MK model predicts a lower initial velocity at an identical condition than the HD model, and leads to slightly poor agreement with the experimental values of initial TPC displacement velocity. A close look at the low-contact-angle region in Figure 7 reveals the similarity of fits for the early stages of the dewetting dynamics for bitumen-treated substrate. For the EC-treated surface, the linear MK model seems being well aligned with the de Gennes HD model in predicting the experimentally determined initial TPC displacement velocity and dynamic contact angle data over the entire dewetting period.

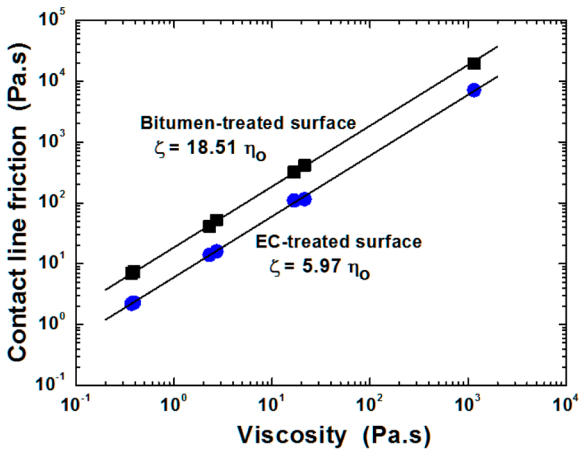

Figure 10. Influence of the viscosity η_o on the contact line friction ζ. The symbols represent the corresponding values of ζ that best fit to the experimental dynamic dewetting data. The solid lines are simple linear correlations fitted to the symbols.

5. CONCLUSIONS

Micropipet technique was successfully developed to study the dewetting of water by emulsified oil drops on clean, bitumen-treated, and EC-treated micro glass spheres. Viscous crude oil drops (0−30% dosage of toluene or naphtha to bitumen) of controlled viscosities and interfacial tensions were used to identify critical physical properties affecting not only dewetting statics but also dynamics. For clean hydrophilic glass surface, no contact angle dynamics were observed, while the equilibrium receding water contact angle decreased with decreasing oil viscosity and interfacial tension achieved by adding an increasing amount of solvent to extra heavy oil of bitumen. For bitumen- and EC-treated glass surfaces, decreasing oil viscosity and interfacial tension led to a significant increase in the change of dynamic receding contact angle. The dewetting dynamics of current systems can be well fitted by either the de Gennes viscous dissipation hydrodynamic model or the Blake/Haynes molecular-kinetic theory. Despite the difficulty in defining which model is best appropriate by curve fitting, applying the two models to the current system uniformly revealed that intrinsic wettability of solid surface and the interfacial tension to viscosity ratio of spreading liquids are the two most critical physicochemical properties in controlling the dynamic dewetting characteristics.

■ ASSOCIATED CONTENT

Supporting Information

Three video clips showing the recorded oil−solid contact experiments and the dewetting processes of water by an emulsion viscous oil drop on solids with three different surface treatments, clean, bitumen-treated, and ethyl cellulose-treated micro glass spheres, respectively. This material is available free of charge via the Internet at http://pubs.acs.org.

AUTHOR INFORMATION

Corresponding Author

*Tel.: (780) 492-7667. Fax: (780) 492-2881. E-mail: zhenghe.xu@ualberta.ca.

Notes

The authors declare no competing financial interest.

ACKNOWLEDGMENTS

This research was conducted under the auspices of the Natural Sciences and Engineering Research Council (NSERC)-Industrial Research Chair (IRC) Program in Oil Sands Engineering. Partial support (Z.X.) by the National Science Foundation of China (grant no. 21333005) for this work is also acknowledged.

REFERENCES

(1) Morrow, N. R. Wettability and its Effect on Oil Recovery. *J. Pet. Technol.* **1990**, *42*, 1476−1484.

(2) Freer, E. M.; Svitova, T.; Radke, C. J. The Role of Interfacial Rheology in Reservior Mixed Wettability. *J. Pet. Sci. Eng.* **2003**, *39*, 137−158.

(3) Rao, D. N. Measurements of Dynamic Contact Angles in Solid-Liquid-Liquid Systems at Elevated Pressures and Temperatures. *Colloids Surf., A* **2002**, *206*, 203−216.

(4) Kolev, V. L.; Kochijashky, I. I.; Danov, K. D.; Kralchevsky, P. A.; Broze, G.; Mehreteab, A. Spontaneous Detachment of Oil Drops from Solid Substrates: Governing Factors. *J. Colloid Interface Sci.* **2003**, *257*, 357−363.

(5) Kocherginsky, N. M.; Tan, C. L.; Lu, W. F. Demulsification of Water-in-Oil Emulsions via Filtration through a Hydrophilic Polymer Membrance. *J. Membr. Sci.* **2003**, *220*, 117−128.

(6) Brinks, B. P.; Lumsdon, S. O. Effects of Oil Type and Aqueous Phase Composition on Oil-Water Mixtures Containing Particles of Intermediate Hydrophobicity. *Phys. Chem. Chem. Phys.* **2000**, *2*, 2959−2967.

(7) Kobayashi, I.; Nakajima, M.; Mukataka, S. Preparation Characteristics of Oil-in-Water Emulsions Using Differently Charged Surfactants in Straight-through Microchannel Emulsification. *Colloids Surf., A* **2003**, *229*, 33−41.

(8) Frisch, T.; Thoumine, O. Predicting the Kinetics of Cell Spreading. *J. Biomech.* **2002**, *35*, 1137−1141.

(9) Guy, D. W.; Crawford, R. J.; Mainwaring, D. E. The Wetting Behavior of Several Organic Liquids in Water on Coal Surfaces. *Fuel* **1996**, *75*, 238−242.

(10) Wang, X.; Nguyen, A. V.; Miller, J. D. Selective Attachment and Spreading of Hydroxamic Acid-Alcohol Collector Mixtures in Phosphate Flotation. *Int. J. Miner. Process.* **2006**, *78*, 122−130.

(11) Takamura, K.; Chow, R. S. A Mechanism for Initiation of Bitumen Displacement from Oil Sand. *J. Can. Pet. Technol.* **1983**, *6*, 22−30.

(12) Masliyah, J.; Czarnecki, J.; Xu, Z. *Handbook on Theory and Practice of Bitumen Recovery from Athabasca Oil Sands, Vol. I: Theoretical Basis*; Kingsley Knowledge Publishing: Canada, 2011.

(13) Kralchevsky, P. A.; Danov, K. D.; Kolev, V. L.; Gurkow, T. D.; Temelska, M. I.; Brenn, G. Detachment of Oil Drops from Solid Surfaces in Surfactant Solutions: Molecular Mechanisms at a Moving Contact Line. *Ind. Eng. Chem. Res.* **2005**, *44*, 1309−1321.

(14) Lim, T. T.; Huang, X. In-Situ Oil/Water Separation Using Hydrophobic-Oleophilic Fibrous Wall: a Lab-Scale Feasibility Study for Groundwater Cleanup. *J. Hazard. Mater.* **2006**, *137*, 820−826.

(15) Blake, T. D.; Haynes, J. M. Kinetics of Liquid/Liquid Displacement. *J. Colloid Interface Sci.* **1969**, *30*, 421−423.

(16) Chertcoff, R.; Calvo, A.; Paterson, I.; Rosen, M.; Hulin, J. P. Transient Effects in Liquid—Liquid Interface Motions through Glass Capillaries. *J. Colloid Interface Sci.* **1992**, *154*, 194−201.

(17) Ramiasa, M.; Ralston, J.; Fetzer, R.; Sedev, R. Contact Line Friction in Liquid-Liquid Displacement on Hydrophobic Surfaces. *J. Phys. Chem. C* **2011**, *115*, 24975−24986.

(18) Cherry, B. W.; Holmes, C. M. Kinetics of Wetting of Surfaces by Polymers. *J. Colloid Interface Sci.* **1969**, *29*, 174−176.

(19) Foister, R. T. The Kinetics of Displacement Wetting in Liquid/Liquid/Solid Systems. *J. Colloid Interface Sci.* **1990**, *136*, 266−282.

(20) Basu, S.; Nandakumar, K.; Masliyah, J. A Study of Oil Displacement on Model Surfaces. *J. Colloid Interface Sci.* **1996**, *182*, 82−94.

(21) Fetzer, R.; Ramiasa, M.; Ralston, J. Dynamics of Liquid-Liquid Displacement. *Langmuir* **2009**, *25*, 8069−8074.

(22) de Ruijter, M. J.; de Coninck, J.; Oshanin, G. Droplet Spreading: Partial Wetting Regime Revisited. *Langmuir* **1999**, *15*, 2209−2216.

(23) Blake, T. D. The Physics of Moving Wetting Lines. *J. Colloid Interface Sci.* **2006**, *299*, 1−13.

(24) de Gennes, P.G. Wetting: Statics and Dynamics. *Rev. Mod. Phys.* **1985**, *57*, 827−863.

(25) de Coninck, J.; de Ruijter, M. J.; Voue, M. Dynamics of Wetting. *Curr. Opin. Colloid Interface Sci.* **2001**, *6*, 49−53.

(26) Neumann, A. W.; Good, R. J. Techniques of Measuring Contact Angles. In *Surface and Colloid Science, Vol. II, Experimental Methods*; Good, R. J., Stromberg, R. R., Eds.; Plenum Press: New York, 1979.

(27) Moran, K.; Yeung, A.; Masliyah, J. Shape Relaxation of an Elongated Viscous Drop. *J. Colloid Interface Sci.* **2003**, *267*, 483−493.

(28) Englert, A. H.; Ren, S.; Masliyah, J.; Xu, Z. Interaction Forces between a Deformable Air Bubble and a Spherical Particle of Tuneable Hydrophobicity and Surface Charge in Aqueous Solutions. *J. Colloid Interface Sci.* **2012**, *379*, 121−129.

(29) Wang, S.; Segin, N.; Wang, K.; Masliyah, J.; Xu, Z. Wettability Control Mechanism of Highly Contaminated Hydrophilic Silica/Alumina Surfaces by Ethyl Cellulose. *J. Phys. Chem. C* **2011**, *115*, 10576−10587.

(30) Yeung, A.; Dabros, T.; Czarnecki, J.; Masliyah, J. On the Interfacial Properties of Micrometer-Sized Water Droplets in Crude Oil. *Proc. R. Soc. A* **1999**, *455*, 3709−3723.

(31) Kistler, S. F. Hydrodynamics of Wetting. In *Wettability*; Burg, J. C., Ed.; Dekker: New York, 1993.

(32) Seveno, D.; Vaillant, A.; Rioboo, R.; Adao, H.; Conti, J.; de Coninck, J. Dynamics of Wetting Revisited. *Langmuir* **2009**, *25*, 13034−13044.

(33) Duvivier, D.; Blake, T. D.; de Coninck, J. Toward a Predictive Theory of Wetting Dynamics. *Langmuir* **2013**, *29*, 10132−10140.

(34) Ranabothu, S. R.; Karnezis, C.; Dai, L. L. Dynamic Wetting: Hydrodynamic or Molecular-Kinetic. *J. Colloid Interface Sci.* **2005**, *288*, 213−221.

(35) Schneemilch, M.; Hayes, R. A.; Petrov, J. G.; Ralston, J. Dynamic Wetting and Dewetting of a Low-Energy Surface by Pure Liquids. *Langmuir* **1998**, *14*, 7047−7051.

(36) Hoffman, R. A Study of the Advancing Interface: I. Interface Shape in Liquid-Gas Systems. *J. Colloid Interface Sci.* **1975**, *50*, 228−241.

(37) Cox, R. G. The Dynamics of the Spreading of Liquids on a Solid Surface: Part 1 Viscous Flow. *J. Fluid Mech.* **1986**, *186*, 169−194.

(38) Hocking, L. M.; Rivers, A. D. The Spreading of a Drop by Capillary Action. *J. Fluid Mech.* **1982**, *121*, 425−442.

(39) Huh, C.; Scriven, L. E. Hydrodynamic Model of Steady Movement of a Solid/Liquid/Fluid Contact Line. *J. Colloid Interface Sci.* **1971**, *35*, 85−101.

(40) de Gennes, P. G. Dynamics of Wetting. In *Liquids at Interfaces*; Charvolin, J., Joanny, J. F., Zinn-Justin, J., Eds.; North-Holland: Amsterdam, 1990.

(41) Mullins, O. C.; Sheu, E. Y. *Structures and Dynamics of Asphaltenes*; Plenum Press: New York, 1998.

(42) Feng, X.; Mussone, P.; Gao, S.; Wang, S.; Wu, S.; Masliyah, J.; Xu, Z. Mechanistic Study on Demulsification of Water-in-Diluted Bitumen Emulsions by Ethylcellulose. *Langmuir* **2010**, *26*, 3050−3057.

(43) Hou, J.; Feng, X.; Masliyah, J.; Xu, Z. Understanding Interfacial Behavior of Ethylcellulose at the Water−Diluted Bitumen Interface. *Energy Fuels* **2012**, *26*, 1740−1745.
(44) Duvivier, D.; Seveno, D.; Rioboo, R.; Blake, T. D.; de Coninck, J. Experimental Evidence of the Role of Viscosity in the Molecular Kinetic Theory of Dynamic Wetting. *Langmuir* **2011**, *27*, 13015−13021.